IEEE Photonics Journal
An IEEE Photonics Society Publication

Open Access

On the Performance of Coherent OFDM Systems in Free-Space Optical Communications

Volume 7, Number 4, August 2015

Yi Wang
Deli Wang
Jing Ma

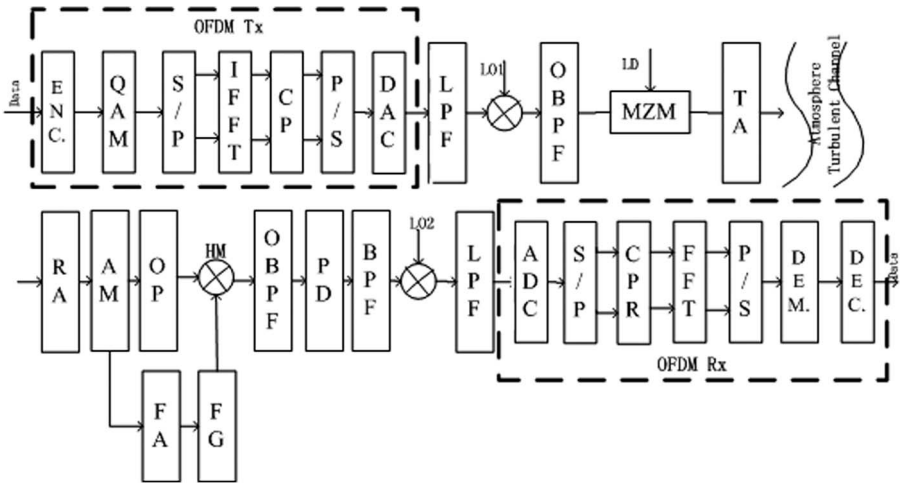

DOI: 10.1109/JPHOT.2015.2450532
1943-0655

IEEE photonics SOCIETY

IEEE

On the Performance of Coherent OFDM Systems in Free-Space Optical Communications

Yi Wang,[1,2] Deli Wang,[1] and Jing Ma[2]

[1]College of Information Engineering, China Jiliang University, Hangzhou 310018, China
[2]National Key Laboratory of Tunable Laser Technology, Harbin Institute of Technology, Harbin 150001, China

DOI: 10.1109/JPHOT.2015.2450532

Manuscript received April 22, 2015; revised June 18, 2015; accepted June 22, 2015. Date of publication June 29, 2015; date of current version July 9, 2015. This work was supported by the State Key Laboratory of Ocean Engineering (Shanghai Jiao Tong University) under Grant 1418, by the China Postdoctoral Science Foundation under Grant 2013M 540290, and by the National Natural Science Foundation of China under Grant 61379027. Corresponding author: Y. Wang (e-mail: wcy16@cjlu.edu.cn).

Abstract: This paper presents a new model of a coherent orthogonal frequency division multiplexing free space optical communication (OFDM-FSO) system that can be tuned with the virtual local oscillator, under the Gamma–Gamma atmospheric turbulence channel, not only considering the intensity scintillation but considering the phase noise caused by atmospheric turbulence effect on the performance of the system as well. The mapping mode of the OFDM signal uses 16-quadrature amplitude modulation (QAM) with better performance. On this basis, we derived the closed form of the symbol error rate and interrupt probability, respectively. In this paper, we analyzed under the premise of the different number of subcarriers, the influence of each parameter of atmospheric channel on the bit error, and the communication interrupt performance of the OFDM-FSO system, respectively. The results show that the coherent OFDM-FSO system can obtain higher sensitivity and can overcome the bad atmosphere influence to obtain good performance of the system.

Index Terms: Orthogonal frequency division multiplexing free space optical communication (OFDM-FSO), coherent detection, atmospheric turbulence channel, symbol error probability, outage probability.

1. Introduction

Free space optical communication (FSO) is considered to be a practical solution to the "last mile problem" in telecommunications. Recently, there has been a resurgence of research interest in this technique, due to its benefits including higher data transmission rates, greater bandwidth, lower power consumption and better security over radio frequency (RF) communications [1], [2]. However, atmospheric attenuation and turbulence due to atmospheric stochastic volatility may lead directly to intensity scintillation and phase fluctuation, which seriously affects stability and reliability when the optical signal of an FSO communication system is transmitted through an atmospheric channel [4].

Orthogonal frequency division multiplexing (OFDM) technology can not only produce higher data transmission rates, but also can effectively suppress inter symbol interference (ISI), due to its increased robustness against frequency selective fading and narrow-band interference, and

high utilization of the frequency spectrum, which can prevent the random fading effect caused by the atmospheric channel, which gradually appears within FSO systems [5], [6]. Recent research on OFDM technology in the FSO communication field has mainly focused on the direct detection method. There are two main areas of research. The first area of research is the BER performance of the OFDM-FSO system in the Gamma–Gamma channel or logarithmic channel, which is affected by the subcarrier modulation method and modulation order at different turbulence intensity levels [7]–[9]. The second area focuses on introduction of technologies that can optimize the performance of OFDM-FSO systems [10], [11].

Researches on coherent detection method are more than direct detection for an OFDM-FSO system, such as the coherent OFDM-FSO transmission system proposed by Vishal Sharma of India Shaheed Bhagat Singh National University of science and technology in 2014, who compared the optical double sideband modulation (ODSB) scheme with the optical single side band modulation (OSSB) scheme. It was found that compared with the direct detection method, coherent detection can reduce the link loss by 1 dB while achieving the same bit error rate [12]. In 2014, Chen *et al.* of Singapore Nanyang Technology University proposed non-equalization orthogonal frequency division multiplexing (NE-OFDM) technology in an FSO communication system, which uses a channel model based on modified Rician distribution, coding and modulation using M-ary differential phase shift keying (MDPSK) method. NE-OFDM technology can reduce the complexity of system design [13]. However, both of these studies did not consider the important issue of coherent detection, which ensures that the frequency stability of the signal light and the local oscillator light at least reach an order of magnitude of 10^{-11} [14].

In this paper, we use a model to describe the turbulence intensity of the Gamma–Gamma atmospheric turbulence channel, and propose a new tunable optical coherent OFDM-FSO system, which considers not only the intensity fluctuation but the phase error caused by the effect of atmospheric turbulence on the performance of the system as well.

2. System Model

2.1. Atmospheric Turbulence Model

In an FSO channel, the strength of an optical wave propagating in a turbulent atmosphere will fluctuate up and down due to refractivity fluctuations, and its weak-strong turbulence intensity fluctuation probability distribution model conforms to a Gamma–Gamma distribution. The Gamma–Gamma model describes the atmospheric fluctuation phenomena including the inner scale and outer scale, and is the product of two independent random processes, each of which has a gamma probability density function (PDF). Therefore, the PDF of the light intensity fluctuation can be described by [3]

$$f(I) = \frac{2(\alpha\beta)^{\frac{(\alpha+\beta)}{2}}}{\Gamma(\alpha)\Gamma(\beta)} I^{\frac{(\alpha+\beta-2)}{2}} \mathrm{K}_{\alpha-\beta}\left(2\sqrt{\alpha\beta I}\right), \qquad I > 0 \tag{1}$$

where I is the normalized signal intensity scintillation, $\Gamma(\cdot)$ is the Gamma function, and $K_n(\cdot)$ denotes a modified Bessel function of the second kind of order n. The positive parameters α and β represent the large-scale and small-scale optical wave intensity scintillation, whose expressions are [3]

$$\alpha = \left\{ \exp\left[\frac{0.49\delta_R^2}{\left(1 + 1.11\delta_R^{\frac{12}{5}}\right)^{\frac{7}{6}}} \right] - 1 \right\}^{-1}, \quad \beta = \left\{ \exp\left[\frac{0.51\delta_R^2}{\left(1 + 0.69\delta_R^{\frac{12}{5}}\right)^{\frac{5}{6}}} \right] - 1 \right\}^{-1}. \tag{2}$$

In the formula, $\delta_R^2 = 1.23 C_n^2 k^{7/6} L^{11/6}$ is the Rytov variance, which can be used to estimate the optical fluctuation intensity. δ_R represents the turbulence intensity, which corresponds to the

logarithmic light intensity fluctuation variance, $k = 2\pi/\lambda$ is the wave number, L is the length of the link, and C_n^2 is the atmospheric structure constant of the refractive index. When $\delta_R^2 < 1$, this indicates weak turbulence, when $\delta_R^2 \cong 1$ this indicates medium turbulence, and when $\delta_R^2 > 1$ this indicates strong turbulence. In addition, based on α and β the flicker factor can be defined by [4]

$$SI = \frac{1}{\alpha} + \frac{1}{\beta} + \frac{1}{\alpha\beta} \tag{3}$$

Due to the random nature of the turbulence communication link, the phase noise caused by atmospheric turbulence is random; therefore, the probability density function of this random noise can be described by a Gaussian distribution with zero mean value [3]. Since the phase noise due to the laser linewidth also satisfies a Gaussian distribution, the distribution model of the phase noise φ caused by atmospheric turbulence can be expressed by [1], [2]

$$f_\varphi(\varphi) = \frac{1}{\sqrt{2\pi}\delta} e^{-\varphi^2/2\delta^2} \tag{4}$$

where δ^2 is the variance of the phase error.

2.2. Tunable Optical Coherent OFDM System Analysis

The tunable optical coherent OFDM-FSO system presented in this article consists of two components, the transmission and receiving sub-systems, as shown in the figure box OFDM Tx and OFDM Rx represent the OFDM signal transmission and receiving sub-systems, respectively. Data encoded by the OFDM Tx uses a 16 quadrature amplitude modulation (QAM) mapping mode to give better performance, which uses a serial-to-parallel conversion (S/P) to transform the data flow into a parallel low speed data stream. The parallel data is allocated to one of a number of N orthogonal subcarriers for parallel transmission. In the frequency domain, each channel is divided into multiple orthogonal and overlapping sub-channels. Each channel uses subcarrier modulation, and the carrier sub-channels are orthogonal to each other for parallel transmission. After the serial-to-parallel conversion, the sequence modulation information $c(n)$, $c(n)$ is formed using IFFT. The OFDM modulated signal of the time domain sampling sequence is calculated including a protection interval. After S/P transformation, the serial sequence is transformed from D/A to obtain the OFDM modulated signal time domain waveform. A low-pass filter (LPF) is used to filter out high frequency noise, and the OFDM signal is then indirectly modulated on a suitable medium frequency f_{LO1}. By then adding a modulated medium frequency signal through the Mach–Zehnder modulator (MZM) on the optical carrier. The signal is emitted by the transmitting antenna (TA) to the atmospheric channel.

The receiving antenna (RA) receives the signal at the other end of the channel. the existing models of coherent detection system are external local oscillator, such as in [12] and [13], which is difficult to guarantee the signal light and the local oscillation light frequency stability are both at least 10^{-11}, in order to ensure that the matching problem of wave shape, amplitude, phase and polarization between the local oscillation light and signal light can be solved. We propose a new model, the local oscillation light is taken from signal light, as shown in Fig. 1, the received light divides into two paths, One path is used as the signal light, and the other as the virtual local oscillation light after amplifying and adjusting the frequency. Fiber grating (FG) has the advantages of good wavelength selectivity, insensitivity to nonlinear effects, insensitivity to polarization, a large bandwidth range and small additional loss. Therefore, we chose optical fiber grating to provide a larger tuning frequency range, which also has the benefit that the tunable frequency can be changed based on the frequency variation of the transmitted signal to ensure better frequency stability of the virtual local oscillator light. An optical fiber amplifier (FA) is also used in the system to ensure that the local oscillator signal has sufficient power, so that the local oscillator signal from the system's light signal in this article can use the coherent detection method to achieve the ideal state. After mixing, we use OBPF to filter out the DC and

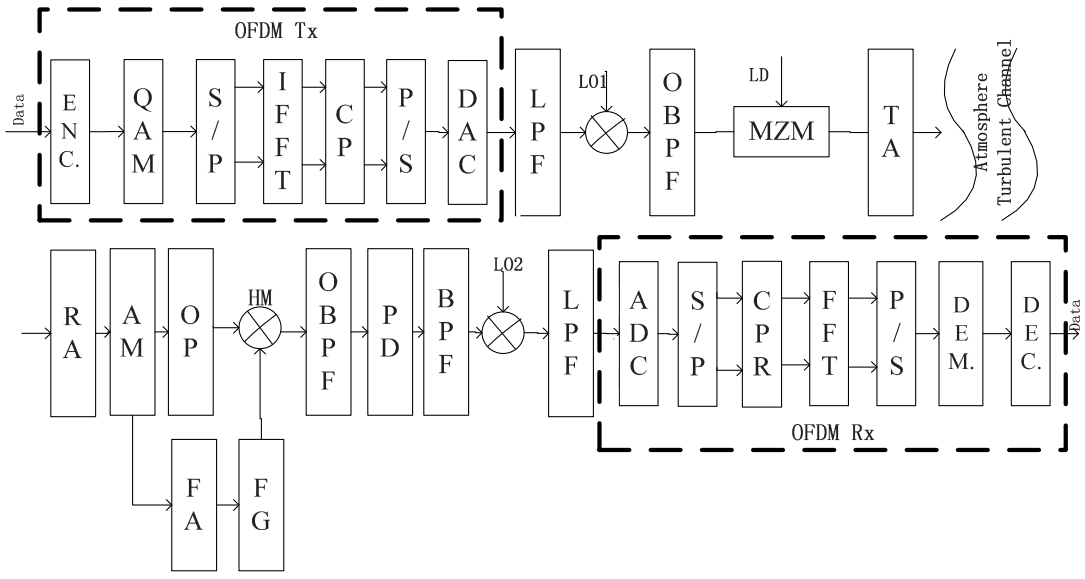

Fig. 1. Block diagram of the tunable virtual optical local oscillator coherent OFDM system over FSO links with Gamma–Gamma channel. ENC (encoder); QAM (quadrature amplitude modulation); S/P (serial-to-parallel conversion); IFFT (Inverse Fast Fourier Transform); CP (cyclic prefix); P/S (parallel-to-serial conversion); DAC (digital to analog converter); LPF (low pass filter); OBPF (optical band pass filer); LD (laser diode); MZM (Mach–Zehnder modulator); TA (transmitting antenna); RA (receiving antenna); HM (heterodyne mixer); AM (amplifier); OP (optical processor); FA (fiber amplifier); FG (fiber grating); PD (photo detector); BPF (band pass filer); FFT (Fast Fourier Transform); CPR (CP removal); DEM. (demodulation); DEC. (decoder).

high frequency components, we obtain the output response current by means of photo detector (PD), the OFDM symbol through the mixer is demodulated and judgment. The LPF is to extract the useful data. As shown in the figure, the OFDM Rx process is the reverse process used by the OFDM Tx, although the spectrum aliasing and subcarrier orthogonality ensures that each channel is still isolated from other sub-channels. The original signal is finally demodulation decoded.

3. Performance Analysis

When receiving, the signal can be represented as

$$E_s(t) = P_T \cdot \mu \cdot \frac{1}{N} \cdot \exp(j2\pi f_{LO1} t) \sum_{i=1}^{\infty} \sum_{k=1}^{N} X_{i,k} \exp(j2\pi f_k t) = m \sum_{i=1}^{\infty} \sum_{k=1}^{N} X_{i,k} \exp[j(\omega_0 t + \varphi_0)] \quad (5)$$

where $X_{i,k}$ represents the signal for the ith OFDM symbol and kth subcarrier. Then, it is assumed that the form of the virtual optical local oscillator is

$$E_L(t) = n \sum_{i=1}^{\infty} \sum_{k=1}^{N} Y_{i,k} \exp[j(\omega_L t + \varphi_L)]. \quad (6)$$

After mixing, the signals can be represented by $E_c^2(t) = E_s^2(t) + E_L^2(t)$, and the output response current PD is $I_R \propto E_c^2(t)$. The DC and high frequency components are filtered out, and the current of the intermediate frequency signal can be obtained by considering the phase noise $\Delta\varphi$, light intensity, and the local oscillator light and the signal light after mixing by the photoelectric detector

$$i(t) = 2R\sqrt{P_0 P_L} I(t) \cos(\Delta\varphi) \cos(\omega_{\mathrm{IF}} t + \varphi_0 - \varphi_L) \quad (7)$$

where P_0 and P_L are power of signal and the virtual optical local oscillator, φ_0 and φ_L are phase of signal and the virtual optical local oscillator. R is the equivalent load resistance, $\omega_{\mathrm{IF}} = \omega_0 - \omega_L$

is the intermediate frequency, and a receiver band pass filter is used to filter out frequencies beyond the range of frequency response of light detector so that band-pass filter bandwidth can be controlled within the scope of the intermediate frequency signal to detect the difference frequency signal, including all of the information carried by the signal light, using (7).

3.1. Symbol Error Rate Analysis

We firstly consider the influence of the average SNR on the system symbol error rate. The part after photoelectric detector of the free space coherent optical communication system is an ideal band-pass filter, the system noise can be described by

$$N_0 = 2q\rho(P_0 + P_L)R^2 + 4K_b T_{\text{sys}} R \tag{8}$$

where q is the electric charge, ρ is the detector efficiency, K_b is the Boltzmann constant, and T_{sys} is the system relative Kelvin temperature. The signal-to-noise ratio can be expressed as

$$\text{SNR} = \frac{4R^2 P_0 P_L I^2(t)\cos^2(\Delta\phi)}{2q\rho(P_0 + P_L)R^2 + 4K_b T_{\text{sys}} R}. \tag{9}$$

Usually, provided there is large enough local light power in the coherent optical communication, the SNR reaches the shot noise limit. Therefore, when P_L is much greater than P_0, we define the magnitude of SNR as $\overline{\text{SNR}}$, $\overline{\text{SNR}} = 2P_0 I^2 \cos^2(\Delta\phi)/q\rho$ and letting $\overline{\gamma} = 2P_0/q\rho$, then $\overline{\text{SNR}} = \overline{\gamma} I^2 \cos^2(\Delta\phi)$. We can then write the system symbol error rate as

$$P_S = hQ\left(\sqrt{\overline{\gamma} I^2 \cos^2(\Delta\varphi)\frac{3TB}{N(M-1)}}\right) \tag{10}$$

where $h = 4$ for 16 QAM. T is the symbol period, B is the OFDM bandwidth, N is the number of subcarriers, and M is constellation mapping coefficient. As $Q(\sqrt{2}\alpha) = 0.5\text{erfc}(\alpha)$, the average symbol error probability in the Gamma–Gamma channel can be expressed as

$$P_{s,\text{OFDM}} = \int_0^{\infty}\int_{-\infty}^{\infty} P_s f_I(I) f_\varphi(\varphi)\, d\varphi\, dI \tag{11}$$

$K_{\alpha-\beta}(2\sqrt{\alpha\beta I}) = (1/2)G_{0,2}^{2,0}[\alpha\beta I\big|_{(\alpha-\beta)/2,-((\alpha-\beta)/2)}^{-}]$, $\text{erfc}\sqrt{x} = (1/\sqrt{\pi})G_{1,2}^{2,0}[x|_{0,0.5}^{1}]$ and a generalization of the classical Meijer's integral can be used for the two G functions [15]. Substituting (1), (4), and (10) into (11) and taking into consideration the scintillation and phase noise in the OFDM-FSO system, the average symbol error rate expressions for the closed form can be written as

$$\begin{aligned} P_{s,\text{OFDM}} &= \frac{h(\alpha\beta)^{\frac{\alpha+\beta}{2}}}{2\pi\Gamma(\alpha)\Gamma(\beta)}\sum_{i=1}^{n} w(x_i)\int_0^{\infty} I^{\frac{\alpha+\beta}{2}-1} G_{1,2}^{2,0}\left[\frac{1}{2}\overline{\gamma} I^2\cos^2\varphi\frac{3TB}{N(M-1)}\middle|\begin{matrix}1\\0,\frac{1}{2}\end{matrix}\right] G_{0,2}^{2,0}\left[\alpha\beta I\middle|\begin{matrix}-\\\frac{\alpha-\beta}{2},\frac{\beta-\alpha}{2}\end{matrix}\right] dI \\ &= \frac{h2^{\alpha+\beta-3}}{\pi^{\frac{3}{2}}\Gamma(\alpha)\Gamma(\beta)}\sum_{i=1}^{n} w_i G_{5,2}^{2,4}\left[\frac{24\overline{\gamma}\cos^2(\sqrt{2}\sigma x_i)TB}{N(M-1)(\alpha\beta)^2}\middle|\begin{matrix}\frac{1-\alpha}{2},\frac{2-\alpha}{2},\frac{1-\beta}{2},\frac{2-\beta}{2},1\\0,\frac{1}{2}\end{matrix}\right] \end{aligned} \tag{12}$$

where n is the approximation order, and $x_i (i = 1, 2, \ldots, n)$ and $w_i (i = 1, 2, \ldots, n)$ are zero and the weights of an nth-order Hermite polynomial.

3.2. Outage Probability Analysis

The transmission reliability of the OFDM system can be verified from calculation of the outage probability. If the system error rate is greater than the target bit error rate, i.e., the probability of

the system SNR is below a target SNR threshold value, then formula (9) gives $E_S/N_0 = \rho P_0 I^2 \delta^2 T/2qBN$, and the value size of the SNR threshold μ will influence the system outage probability

$$P_{\text{out}} = \Pr\left(\frac{E_s}{N_0} \le \mu\right) = \Pr\left(\frac{\rho P_0 I^2 \delta^2 T}{2qBN} \le \mu\right) = \int_0^{\frac{1}{\delta}\sqrt{\frac{2\mu qBN}{\rho P_0 T}}} f(I)\, dI. \tag{13}$$

Let $x = \sqrt{2\mu qB/\rho P_0}$ for the normalized threshold value, and then, the closed form expression for the outage probability is

$$P_{\text{out}} = \frac{(\alpha\beta)^{\frac{(\alpha+\beta)}{2}}}{\Gamma(\alpha)\Gamma(\beta)} \left(\frac{x}{\delta}\sqrt{\frac{N}{T}}\right)^{\frac{\alpha+\beta}{2}-1} G_{1,3}^{2,1}\left[\alpha\beta\frac{x}{\delta}\sqrt{\frac{N}{T}}\middle| \begin{matrix} 1-\frac{\alpha+\beta}{2} \\ \frac{\alpha-\beta}{2}, \frac{\beta-\alpha}{2}, \frac{-\alpha-\beta}{2} \end{matrix}\right] \tag{14}$$

4. Simulation and Numerical Analysis

In this section, we use simulation and numerical analysis to verify that the scintillation intensity and phase fluctuation influence the performance of the tunable optical coherent OFDM-FSO system under different numbers of subcarriers. This paper uses weak, moderate and strong turbulence intensities at different Rytov variance values $\delta_R^2 = 0.49$, $\delta_R^2 = 1.21$, $\delta_R^2 = 4$. The turbulence intensity under different scintillation parameters are $\{\alpha = 6.05, \beta = 4.47, SI = 0.43\}\{\alpha = 4.19, \beta = 2.26, SI = 0.79\}\{\alpha = 4.34, \beta = 1.31, SI = 1.17\}$ respectively [2], based on (2) and (3).

Each turbulence intensity level exhibits different phase noise, and thus has a different impact on the system performance. The phase fluctuation parameters are $\delta^2 = 0.085\pi$ and $\delta^2 = 0.25\pi$ in this paper as given by [2], which correspond to weak and strong phase fluctuations respectively with different turbulence intensity levels. The number of subcarriers has a strong influence on the performance of the OFDM-FSO system, and increasing the number of subcarriers can increase the channel capacity, enabling transmission of more data at the same rate. However, increasing the number of subcarriers, leads to an unacceptably high peak to average power ratio (PAPR) of the multi carrier signal [16], [17]. Taking into consideration the PAPR limit, device constraints and other conditions, the number of subcarriers used this paper is $N = 128$, 256, and 1024.

Fig. 2 shows the simulation and analysis of the relationship between the average signal-to-noise ratio and the symbol error rate. As shown for each value of N, if the average SNR is known, then as the light intensity scintillation and phase fluctuation due to atmospheric turbulence increases, the symbol error rate of the system also increases. As the number of subcarriers increases, the system symbol error rate also increases. For example, when SI $= 0.43$ and $\delta^2 = 0.085\pi$, the best symbol error probability performance is 1.58×10^{-11}, 1.54×10^{-10}, and 2.29×10^{-9} for $N = 128$, 256, and 1024, respectively. Under different scintillation intensity levels, there the phase noise shows different influences on the symbol error rate of the system. Comparison of charts (a) (b) (c) of weak and strong phase noise shows that for the same average signal-to-noise ratio, the effect of the phase noise on the symbol error rate is greatest where there is weak turbulence, the system symbol error rate was less affected by phase noise where there is medium turbulence or strong turbulence. At the same time, the symbol error rate in the weak phase noise can be higher three, two and one order of magnitude than strong phase noise in the strong, medium and weak turbulence intensity for the same average signal-to-noise ratio.

For a more comprehensive analysis of the system symbol error rate performance and the sensitivity performance simulation, we analyzed the relationship between the symbol error and the required average received optical power for different atmospheric turbulence intensity levels. Once the system design is fixed, we can study the effects of each parameter on the performance of the system under random variation of the atmospheric channel, for a fixed number of subcarriers. Taking into consideration the effect of the number of subcarriers on the performance of the

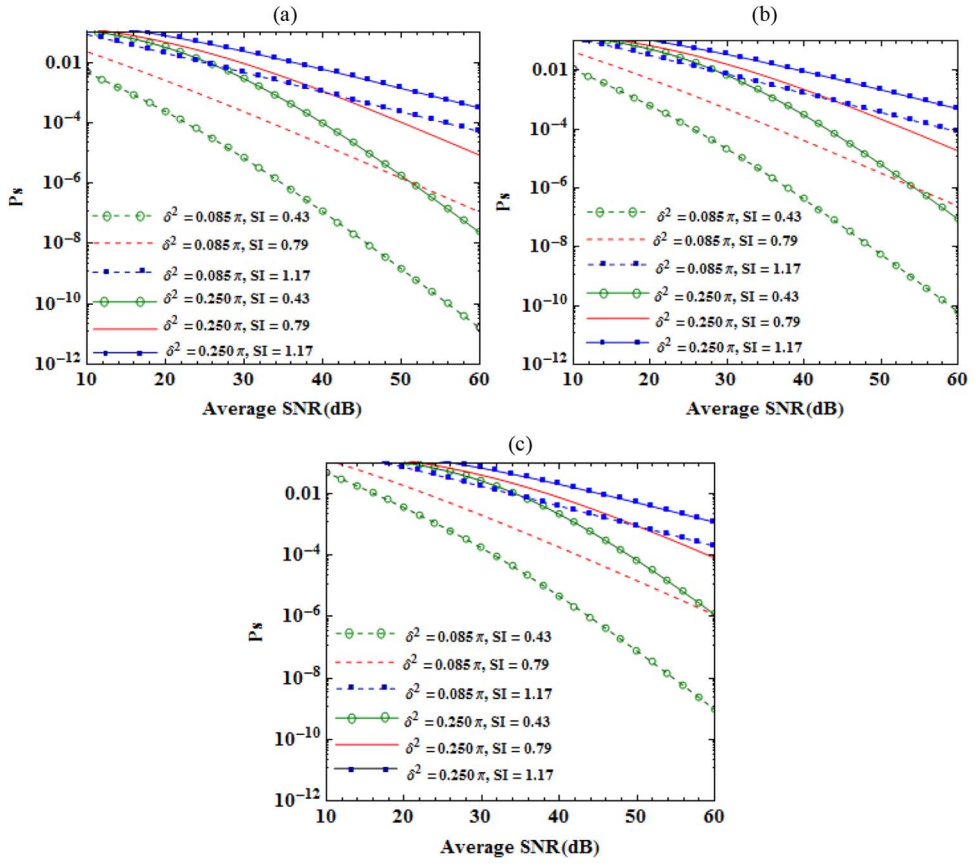

Fig. 2. Symbol error probability performance of the coherent OFDM system as a function of average SNR for different numbers of subcarriers (a) $N = 128$, (b) $N = 256$, and (c) $N = 1024$.

system, we choose the number of subcarriers $N = 256$. To generate the theoretical curves, the electrical bandwidth value was set at $B = 10$ GHz, and the equivalent system temperature (Kelvin) in atmospheric turbulence channel was assumed to be $T = 300$ K.

As shown in Fig. 3, the system symbol error rate using the coherent detection mode was significantly lower than the direct detection method in different atmospheric turbulence conditions. The symbol error rate of the OFDM-FSO system decreased as the required average received optical power increased. The system symbol error rate under weak phase fluctuation conditions was lower than under strong phase fluctuations when the required average received power was certain. Combining graphs (a)–(c) showed that as the intensity scintillation and phase fluctuation increased, the average received optical power was also required to increase in order for the system to reach a certain symbol error rate. This means that there should be a corresponding increase in the transmission power of the system. In addition, the figure shows that with strong atmospheric turbulence conditions, the effect of the phase noise on the system sensitivity is smaller than with weak turbulence. If direct detection is used, when the symbol error rate reaches 10^{-6}, then the required average received optical power for weak turbulence conditions are -54.1 dBm and -52.6 dBm when $\delta^2 = 0.085\pi$ and $\delta^2 = 0.25\pi$ respectively, as shown in Fig. 3(a). However, using coherent detection method, the required average received optical powers with the same parameters are -57.9 dBm and -56.5 dBm. This illustrates that the use of the coherent detection method has higher sensitivity than the direct detection method, and that the sensitivity will be 3–4 dBm higher for the same error cases. For medium and strong turbulence, the situation is similar. Meanwhile the required average received optical power for strong phase noise is 2–4 dBm higher than weak phase noise cases to achieve the same symbol error rate.

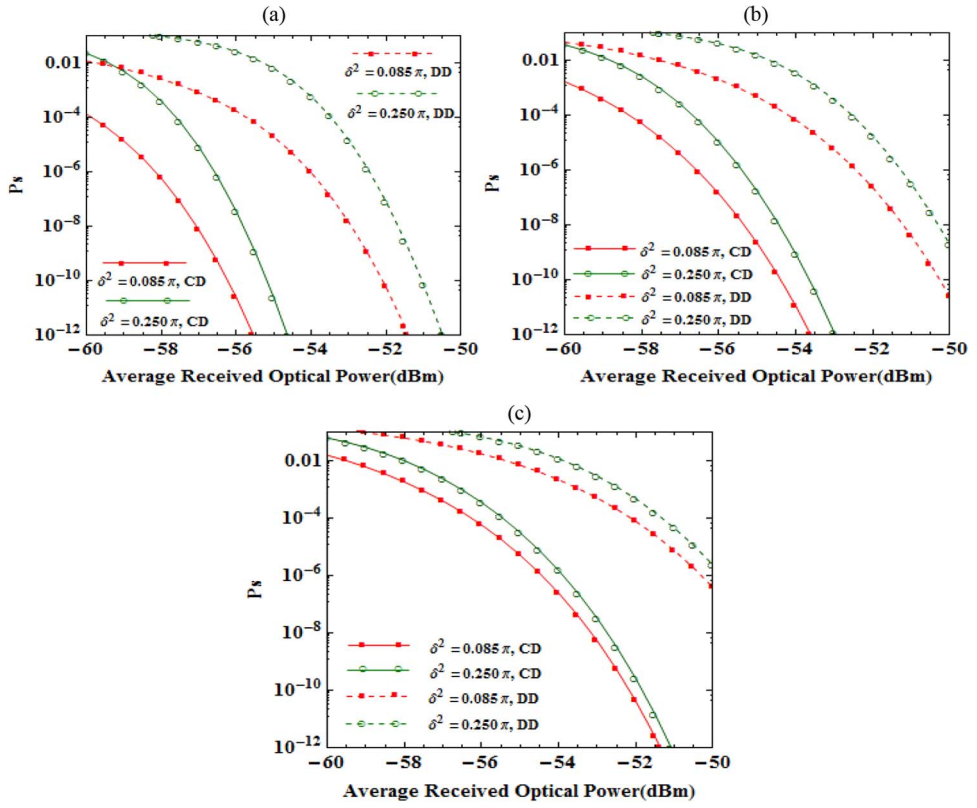

Fig. 3. Symbol error probability performance of the coherent OFDM system as a function of average received optical power for different turbulent channel (a) SI = 0.43, (b) SI = 0.79, and (c) SI = 1.17. CD = coherent detection, DD = direct detection.

Simulation and analysis of the system communication interruption probability were performed to verify the reliability of the OFDM system, as shown in Fig. 4(a)–(c), represent the communication interruptions of the OFDM-FSO system when the number of subcarriers was $N = 128$, 256, and 1024. Raising the intensity scintillation and phase fluctuation will cause a significantly increased outage probability, At the same time, the outage probability decreases while reducing the normalized threshold value. The more the number of subcarriers, the faster the outage probability of the system increases with the increase of the normalized threshold values. for example, with the normalized threshold increasing from -20 dB to -10 dB conditional on a phase noise of $\delta^2 = 0.25\pi$ the outage probability in Fig. 4(a) $N = 128$ rises to 0.040, and it rises to 0.060 and 0.135 in Fig. 4(b) $N = 256$ and Fig. 4(c) $N = 1024$. It should be noted that the probability of interrupted communication is almost one hundred percent when the normalized thresholds are greater than 10 dB in the three cases. The stability of the system can be improved by preferably controlling the threshold value. Comparison of Fig. 4(a)–(c) shows that under the same conditions, the system communication interruption probability increases as the number of subcarriers increases. This is because when the total transmission rate and required bandwidth of the OFDM system are approximately constant, the adjacent subcarrier spacing becomes small as the number of subcarriers increases, which will exacerbate the interference between adjacent subcarriers and, thus, improve the communication interruption probability.

5. Conclusion

This paper combines the advantages of OFDM technology and coherent detection, and proposes a type of new model that can be tuned with the virtual local oscillator for a coherent detection OFDM-FSO system. We derived the closed-form expressions of the system symbol error

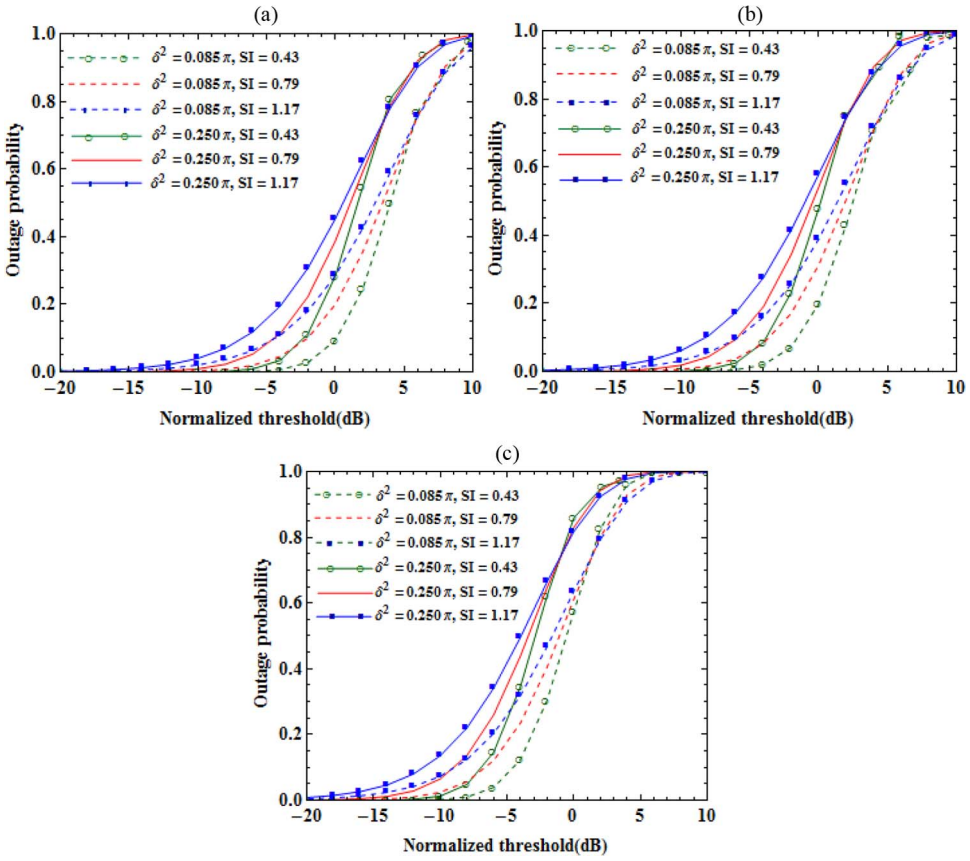

Fig. 4. Outage probability of the coherent OFDM system as a function of normalized threshold for different numbers of subcarrier (a) $N = 128$, (b) $N = 256$, and (c) $N = 1024$.

rate and outage probability in a Gamma–Gamma atmospheric turbulence channel. We analyzed the influence of the scintillation intensity, phase noise due to atmospheric turbulence and the number of subcarriers on the system performance. The conclusions are as follows: under the same atmospheric environment, the symbol error rate of the system increases as the number of subcarriers increases. As the scintillation intensity increases, the effects of phase noise on the system symbol error rate and sensitivity are small. The symbol error rate and the receiving sensitivity using coherent detection method is better than the direct detection method. The system has a larger possibility of communication interruption only where there are a large number of subcarriers and strong phase fluctuations. In recent years, research on OFDM-FSO systems has focused on direct detection rather than on coherent detection methods. Therefore, this paper provides a theoretical reference to study coherent detection OFDM-FSO systems applied in the field of free space optical communication.

References

[1] W. Gappmair and M. Flohberger, "Error performance of coded FSO links in turbulent atmosphere modeled by Gamma–Gamma distribution," *IEEE Trans. Wireless Commun.*, vol. 8, no. 5, pp. 2209–2213, May 2009.
[2] G. Xie, F. Wang, A. Dang, and H. Guo, "A novel polarization multiplexing system for free-space optical links," *IEEE Photon. Technol. Lett.*, vol. 23, no. 20, pp. 1484–1486, Oct. 2011.
[3] M. A. Al-Habash, L. C. Andrews, and R. L. Phillips, "Mathematical model for the irradiance probability density function of a laser beam propagating through turbulent media," *Opt. Eng.*, vol. 40, no. 8, pp. 1554–1562, 2001.
[4] Y. Wang and F. Du, "Employing circle polarization shift keying in free space optical communication with gamma–gamma atmospheric turbulence channel," *Opt. Commun.*, no. 333, pp. 167–174, Aug. 2014.
[5] T. Ohtsuki, "Multiple subcarrier modulation in optical wireless communications," *Opt. Wireless Commun.*, vol. 41, no. 3, pp. 74–79, Mar. 2003.

[6] N. Cvijetie, D. Qian, and T. Wang, "10 Gb/s free space optical transmission using OFDM," presented at the Nat. Fiber Optic Eng. Conf., San Diego, CA, USA, Feb. 24–28, 2008.
[7] N. Cvijetic, "WiMAX access using optical wireless technology with heterodyne detection in turbulent atmospheric channels" presented at the Global Telecommun. Conf., San Francisco, CA, USA, Nov. 26–Dec. 1, 2006.
[8] A. Bekkali and C. Ben Naila, "Transmission analysis of OFDM-based wireless services over turbulent radio-on-FSO links modeled by gamma–gamma distribution," *IEEE Photon. J.*, vol. 2, no. 3, pp. 510–520, May 2010.
[9] H. E. Nistazakis, A. N. Stassinakis, H. G. Sandalidis, and G. S. Tombras, "QAM and PSK OFDM RoFSO over M-turbulence induced fading channels," *IEEE Photon. J.*, vol. 7, no. 1, Feb. 2015, Art ID. 7900411.
[10] S. Chaudharya, A. Amphawanab, and K. Nisar, "Realization of free space optics with OFDM under atmospheric turbulence," *Optik*, vol. 125, no. 18, pp. 5196–5198, Sep. 2014.
[11] F. Bai, Y. Su, and T. Sato, "Performance evaluation of dual diversity reception base on OFDM RoFSO systems over correlated log-normal fading channel," presented at the ITU Kaleidoscope Academic Conf., St. Petersburg, Russia, Jun. 3–5, 2014, pp. 263–268.
[12] V. Sharma and Sushank, "High speed CO-OFDM-FSO transmission system," *Optik*, vol. 125, no. 6, pp. 1761–1763, Mar. 2014.
[13] C. Chen, W. Zhong, X. Li, and D. Wu, "MDPSK based non equalization OFDM for coherent free space optical communication," *IEEE Photon. Technol. Lett.*, vol. 26, no. 16, pp. 1617–1620, Aug. 2014.
[14] W. Shich and C. Athaudage, "Coherent optical orthogonal frequency division multiplexing," *Electron. Lett.*, vol. 40, no. 10, pp. 587–588, May 2006.
[15] Wolfram Function Site, 2014. [Online]. Available: http://functions.wolfram.com/
[16] R. W. Bauml, R. F. H. Fischer, and J. B. Huber, "Reducing the peak-to-average power ratio of multicarrier modulation by selected mapping," *Electron. Lett.*, vol. 32, no. 22, pp. 2056–2057, Oct. 1996.
[17] J. Armstrong, "Peak-to-average power reduction for OFDM by repeated clipping and frequency domain filtering," *Electron. Lett.*, vol. 38, no. 5, pp. 246–247, Feb. 2002.